Biochemical and cellular characterization of VRX0466617, a novel and selective inhibitor for the checkpoint kinase Chk2

Luigi Carlessi,[1] Giacomo Buscemi,[1] Gary Larson,[2] Zhi Hong,[2] Jim Zhen Wu,[2] and Domenico Delia[1]

[1]Department of Experimental Oncology, Istituto Nazionale Tumori, Milan, Italy and [2]Drug Discovery, Valeant Pharmaceuticals International, Costa Mesa, California

Abstract

VRX0466617 is a novel selective small-molecule inhibitor for Chk2 discovered through a protein kinase screening program. In this study, we provide a detailed biochemical and cellular characterization of VRX0466617. We show that VRX0466617 blocks the enzymatic activity of recombinant Chk2, as well as the ionizing radiation (IR)–induced activation of Chk2 from cells pretreated with the compound, at doses between 5 and 10 μmol/L. These doses of VRX0466617 inhibited, to some extent, the phosphorylation of Chk2 Ser^{19} and Ser^{33-35}, but not of Chk2 Thr^{68}, which is phosphorylated by the upstream ataxia-telangiectasia mutated (ATM) kinase. Interestingly, VRX0466617 induced the phosphorylation of Chk2 Thr^{68} even in the absence of DNA damage, arising from the block of its enzymatic activity. VRX0466617 prevented the IR-induced Chk2-dependent degradation of Hdmx, concordant with the *in vivo* inhibition of Chk2. Analysis of ATM/ATM and Rad3-related substrates Smc1, p53, and Chk1 excluded a cross-inhibition of these kinases. VRX0466617 did not modify the cell cycle phase distribution, although it caused an increase in multinucleated cells. Whereas VRX0466617 attenuated IR-induced apoptosis, in short-term assays it did not affect the cytotoxicity by the anticancer drugs doxorubicin, Taxol, and cisplatin. These results underscore the specificity of VRX0466617 for Chk2, both *in vitro* and *in vivo*, and support the use of this compound as a biological probe to study the Chk2-dependent pathways. [Mol Cancer Ther 2007;6(3):935–44]

Received 9/13/06; revised 12/5/06; accepted 1/30/07.

Grant support: Italian Association for Cancer Research, Italian Ministry of Health (Ricerca Finalizzata), Consiglio Nazionale Ricerche, and Telethon grant GGP05226.

The costs of publication of this article were defrayed in part by the payment of page charges. This article must therefore be hereby marked *advertisement* in accordance with 18 U.S.C. Section 1734 solely to indicate this fact.

Requests for reprints: Domenico Delia, Department of Experimental Oncology, Istituto Nazionale Tumori, Via G. Venezian 1, 20133 Milan, Italy. Phone: 39-2-2390-2641; Fax: 39-2-2390-2764.
E-mail: domenico.delia@istitutotumori.mi.it

doi:10.1158/1535-7163.MCT-06-0567

Introduction

The therapeutic activity of many anticancer agents rests on their capability to induce cell death by damaging DNA, as in the case of cisplatin, Adriamycin, and ionizing radiation (IR). However, the resistance to these agents, either intrinsic or acquired, provides a barrier to efficacious cancer treatment. Studies in recent years have shown that, when treated with genotoxic agents, cells swiftly respond by activating DNA damage checkpoint responses that prompt the repair of DNA lesions while transiently slowing down replication, or elicit an apoptotic program in case of massive or irreparable lesions (1). Key components of this DNA damage response pathway are two phosphoinositol-3 kinase–like protein kinases: ataxia-telangiectasia mutated (ATM) and ATM and Rad3-related (ATR; refs. 1, 2). These nuclear kinases become activated after DNA damage and dynamic interactions with sensory components of the damage such as the Mre11-Rad50-Nbs1 complex. They subsequently phosphorylate several substrates important for DNA repair, cell cycle arrest, transcription, and apoptosis. However, whereas ATM responds to DNA double-strand breaks induced by IR and other radiomimetic drugs, ATR mainly detects single-strand breaks arising from stalled replication forks or in response to UV radiation. In addition, ATM partakes in multiple cell cycle phase checkpoints, whereas ATR is primarily involved in S-phase checkpoint. Downstream phosphorylation targets of ATM and ATR are the effector serine/threonine kinases Chk1 and Chk2, which in turn phosphorylate partially overlapping residues in other target proteins to induce cell cycle arrest and facilitate DNA repair. Whereas Chk1 is activated by ATR phosphorylation on Ser^{317} and Ser^{345}, Chk2 is activated by ATM phosphorylation on Thr^{68} (3).

Downstream targets of Chk2 include Cdc25A and Cdc25C, which, on phosphorylation, undergo degradation and cytoplasmic relocalization, respectively, and induce cell arrest at G_1, S, and G_2-M phases (3). Another important target of Chk2 is p53, the phosphorylation of which on Ser^{20} regulates p53 transcriptional activation. Moreover, the phosphorylation of Hdmx Ser^{367} by Chk2 enhances its degradation (4, 5) and promotes the accumulation of p53 and transcriptional induction of p53-responsive genes. Chk2 also phosphorylates the transcription factor E2F-1 on Ser^{364}, thereby enhancing its stability and promoting apoptosis (6, 7). Other known Chk2 substrates include BRCA1 and promyelocytic leukemia, with their functions implicated in DNA repair and apoptosis, respectively (8, 9).

As alterations of genes of the DNA damage response can modulate the cellular chemo/radiosensitivity, this pathway has been proposed as an attractive pharmacologic target to potentiate the efficacy of chemoradiation protocols (10). In support of this is the identification and development of several small molecules that specifically enhance the

cytotoxicity of DNA-damaging anticancer agents by abrogating checkpoint responses.

One such compound is KU-55933, an inhibitor of ATM, which radiosensitizes and markedly reduces the clonogenic survival of breast carcinoma cells at pharmacological concentrations (11). In preclinical models, it enhances cytotoxicity by IR, bleomycin, etoposide, and doxorubicin (12). 7-Hydroxystaurosporine (UCN-01; ref. 13) is a Chk1 inhibitor that abrogates the S-phase and G_2-M checkpoints and potentiates the killing of cancer cells including those with p53 mutations by agents like cisplatin, camptothecin, and IR. Current phase II clinical trials in patients with advanced ovarian cancer, metastatic melanoma, large-cell lymphoma, and small-cell lung cancer will determine the clinical efficacy of UCN01 (14). The indocarbazole Go6976 is an effective inhibitor of Chk1 and Chk2 that abrogates the S and G_2-M arrest and potentiates the cytotoxicity of a topoisomerase I inhibitor, but only in p53-defective cells (15). CEP-3891 is a highly specific inhibitor of Chk1 that increases tumor cell radiosensitivity and accelerates nuclear fragmentation of cells prematurely progressing through mitosis (16). Recently, a novel class of benzimidazole-based ATP-competitive Chk2 inhibitors has been reported (17). One of these derivatives (compound 2h) can suppress IR-induced T-cell death.

In this study, we provide a detailed biochemical and cellular characterization of a Chk2 selective inhibitor VRX0466617. We show that it blocks the enzymatic activity of Chk2 *in vitro* and *in vivo*, but not that of ATM or Chk1. VRX0466617 does not potentiate the killing by cancer chemotherapeutic agents in short-term assays, although in long-term assays it may attenuate the IR-induced cell death.

Materials and Methods

Cell Lines and Treatments

The EBV-immortalized normal lymphoblastoid cell line LCL-N (18) was cultured in RPMI 1640 supplemented with 15% heat-inactivated FCS. Immortalized normal human foreskin fibroblasts BJ-hTERT were cultured in DMEM plus M199 (4:1 ratio) with 10% FCS. HCT15 and HCT116 colon cancer cell lines were grown in DMEM and McCoy's 5A, respectively, with 10% FCS. HCT116-Chk2$^{-/-}$ (19) were a kind gift of Bert Vogelstein (Howard Hughes Medical Institute, Chevy Chase, MD). SAOS osteosarcoma and MCF7 breast adenocarcinoma cell lines were cultured in DMEM with 10% FCS. Mouse thymocytes were isolated by mechanical disaggregation of thymuses from four 28-week-old mice (a kind gift of Dr. Giacomo Manenti, Department of Experimental Oncology, Istituto Nazionale Tumori, Milan, Italy) and cultured in RPMI 1640 with 15% FCS. Culture media contained penicillin (100 units/mL), streptomycin (100 μg/mL), and glutamine (2 mmol/L). Cells were cultured at 37°C in a 5% CO_2 incubator. VRX0466617 (MW, 447 Da) was synthesized at Valeant Pharmaceuticals (Costa Mesa, CA), stored at −20°C as a 10 mmol/L stock solution in DMSO, and diluted to a maximal final DMSO concentration of 0.1% in the reaction buffer or culture medium. The ATM kinase inhibitor KU-55933 (KuDOS Pharmaceuticals, Cambridge, United Kingdom) and VRX0466617 were added to exponentially growing cells 1 to 2.5 h before irradiation, respectively. Cells were irradiated with an IBL437CO instrument (Oris Industries, Gif-sur-Yvette, France) equipped with a ^{137}Cs source providing 675 cGy/min. Transient transfections of exponentially growing cells seeded on 100-mm plates were done with Trans-Fast reagent (Promega, Madison, WI) according to the manufacturer's instructions. The spectrophotometric measurement of cell viability was done using the 3-(4,5-dimethylthiazol-2-yl)-2,5-diphenyltetrazolium bromide assay (Sigma, St. Louis, MO) and a Tecan (Maennedorf, Switzerland) 96-well plate reader.

Western Blots

Untreated or treated cells were washed with PBS plus 0.1 mmol/L Na_3VO_4 (Sigma), pelleted, and lysed in Laemmli buffer [0.125 mol/L Tris-HCl (pH 6.8), 5% SDS] containing protease and phosphatase inhibitors including 1 mmol/L phenylmethylsulfonyl fluoride, 10 μg/mL pepstatin, 100 kallikrein-inactivating units/mL aprotinin, 10 μg/mL leupeptin (all from Calbiochem, San Diego, CA), and 1 mmol/L Na_3VO_4. After 5-min boiling and sonication, lysates were quantitated by micro-bicinchoninic acid assay (Pierce, Rockford, IL). Aliquots containing 50 μg of protein plus 5% β-mercaptoethanol were size fractionated on 5% or 8% SDS-PAGE and electroblotted onto polyvinylidene difluoride membranes (Millipore, Bedford, Mass.). After blocking with 4% nonfat dried milk in PBS plus 0.1% Tween 20 (Sigma), membranes were incubated with monoclonal antibodies for Chk2 (clone 44D4/21; refs. 18, 20), p53 (clone DO-7), and β-actin (Sigma) and with rabbit antibodies specific for the phosphorylated residues of Chk2 Thr^{387}, Thr^{68}, Ser^{19}, Ser$^{33-35}$; p53 Ser^{15} and Ser^{20}; and Chk1 Ser^{345} (all from Cell Signaling Technology, Beverly, MA). Rabbit antibodies against Smc1 phospho-Ser^{966}, total Smc1, Hdmx, and Chk1 phospho-Ser^{317} were from Bethyl Laboratories (Montgomery, TX). Binding of antibodies to membranes was detected with peroxidase-conjugated secondary antibodies and ECL SuperSignal (Pierce) on autoradiographic films. Bands were acquired with DuoScan system (Agfa, Mortsel, Belgium) and quantitated with ImageQuant software (Molecular Dynamics, Sunnyvale, CA).

Chk2 Immunoprecipitation and Kinase Assay

Cells were lysed for 30 min in ice-cold buffer containing 20 mmol/L Tris-HCl (pH 8), 0.5% NP40, 150 mmol/L NaCl, 1 mmol/L EDTA, 1 mmol/L phenylmethylsulfonyl fluoride, pepstatin (1 μg/mL), leupeptin (2 μg/mL), aprotinin (2 μg/mL), 25 mmol/L NaF, 1 mmol/L EDTA, and 1 mmol/L Na_3VO_4. After treatment with 15 μL of immobilized protein G (Sigma) for 45 min at 4°C, lysates were immunoprecipitated, as described ref. 21, with 5 μg of anti-Chk2 antibody (clone 44D4/21) and 15 μL of immobilized protein G at 4°C for 3 h. The Chk2 kinase activity was assayed at 30°C for 30 min in a 20 μL reaction mixture containing 50 mmol/L HEPES (pH 8.0), 10 mmol/L $MgCl_2$, 2.5 mmol/L EDTA, 1 mmol/L DTT, 10 μmol/L β-glycerophosphate, 1 mmol/L NaF, 0.1 mmol/L Na_3VO_4,

0.1 mmol/L phenylmethylsulfonyl fluoride, 10 μmol/L ATP, and 30 μCi of [γ-^{32}P]ATP, and, when required, glutathione *S*-transferase (GST)-Cdc25C fragment as a substrate. The reaction products were separated by SDS-PAGE, autoradiographed, and Western blotted to verify the amount of immunoprecipitated Chk2 per sample.

In vitro Kinase Assays with Recombinant Chk1 and Chk2

Recombinant human GST-Chk1 and GST-Chk2 proteins were purchased from Upstate (Lake Placid, NY). Assay conditions were based on published protocols with minor modifications. Briefly, 10 nmol/L of Chk1 or Chk2 were used to phosphorylate 25 μmol/L myelin basic protein (Invitrogen, Carlsbad, CA). This reaction took place in a buffer that contained 8 mmol/L MOPS (pH 7.2), 10 mmol/L β-glycerol phosphate, 1.5 mmol/L EGTA, 0.4 mmol/L EDTA, 0.4 mmol/L sodium orthovanadate, 100 μmol/L ATP, 1 μCi [γ-^{33}P]ATP, 15 mmol/L $MgCl_2$, 0.4 mmol/L DTT, 0.006% Brij-35, 1% glycerol, and 0.2 mg/mL bovine serum albumin in a final volume of 25 μL. The reaction was incubated for 30 min at 24°C and was terminated by adding 100 μL of 1% trichloroacetic acid. The quenched solution was incubated for 5 min at room temperature, to allow the protein to precipitate, and then subsequently transferred to a 96-well white GF/B filter plate (Perkin-Elmer, Wellesley, MA) using a Perkin-Elmer Filtermate Universal Harvester. The filter plate was washed 10 times with water, once with ethanol before, and dried. Forty microliters of Microscint (Perkin-Elmer) were added to each well and the radioactivity that was incorporated into myelin basic protein was counted using a Perkin-Elmer TopCount. VRX0466617 was titrated and its IC_{50} values against both Chk1 and Chk2 were determined. The reported IC_{50} values are the average of at least two sets of data. To determine the competitive nature of VRX0466617 with ATP, the compound concentration was varied from 0 to 200 nmol/L whereas ATP was varied from 50 to 500 μmol/L in the assays to assess the ATP effect on inhibition. Prism 4.0 software (GraphPad, San Diego, CA) was used for the IC_{50} determination and Lineweaver-Burk kinetic analysis.

To investigate the inhibition mechanism of VRX0466617, Chk2 assays with a catalytically active recombinant GST-Chk2 (20) were prepared by incubating for 30 min at 30°C with 2 μg of enzyme and 1 μg of GST-Cdc25C substrate in 30 μL of kinase buffer (20 mmol/L Tris-HCl, 75 mmol/L KCl, 5 mmol/L $MgCl_2$, 0.5 mmol/L EDTA, 2 mmol/L DTT, 50 μmol/L ATP, and 15 μCi of [γ-^{32}P]ATP). The reaction products were separated by SDS-PAGE and autoradiographed. The gels were then stained with Coomassie blue to visualize the amount of loaded substrate per lane.

Cell Cycle Phase Analysis

Radiation-induced cell cycle phase modifications were examined by flow cytofluorimetry on propidium iodide–stained cells (22) using a FACSCalibur instrument fitted with a Cell Quest software package (Becton Dickinson, Sunnyvale, CA). G_2-M progression was evaluated as described (23) on SAOS cells and treated with either DMSO (1:1,000) or 10 μmol/L VRX0466617, with or without 10-Gy IR. Chemicals were added 0.5 h before irradiation and samples were harvested 4 h later, fixed, and immunofluorescence labeled with the phospho-Ser^{10} histone H3 antibody (Alexa Fluor 488 Conjugate, Cell Signaling Technology) to detect mitotic cells.

Results

VRX0466617 Inhibits the Catalytic Activity of Chk2 Both *In vitro* and *In vivo*

Through a high-throughput screening of Valeant collection of compound libraries, we discovered a series of compounds with a pharmacophore of 4-cyano-3-hydroxy-5-arylamino-isothiazoles that exhibit potent inhibitory activity against protein kinases (24). Further structure-activity relationship studies modified the core of the molecules to 3-hydroxy-4-carboxyalkylamidino-5-arylamino isothiazole moiety. One of the leads, VRX0466617, was found to possess potent activity against Chk2 (Fig. 1). Using a radioactive-based filter binding assay, we determined its IC_{50} for Chk2 as 120 nmol/L. Interestingly, it does not inhibit the related Chk1 activity in the similar enzymatic assay with IC_{50} > 10 μmol/L. Further kinetic analysis indicates that it is ATP competitive with an inhibition constant (K_i) of 11 nmol/L, suggesting a possible action mechanism of directly binding to the ATP site in Chk2 (25). Therefore, like other ATP-competitive inhibitors, VRX0466617 IC_{50} value is highly influenced by the ATP concentration in the assay. In our case, we used a relatively high concentration of ATP at 100 μmol/L for the assay.

The bacterial recombinant GST-Chk2 fusion protein possesses both *cis* and *trans* phosphorylation activity toward GST-Cdc25C substrate. To further understand the inhibitory mechanism of VRX0466617, *in vitro* kinase reactions were done in the presence of GST-Chk2, GST-Cdc25C, and two different concentrations (10 or 30 μmol/L) of VRX0466617. From SDS gel analysis, these concentrations of VRX0466617

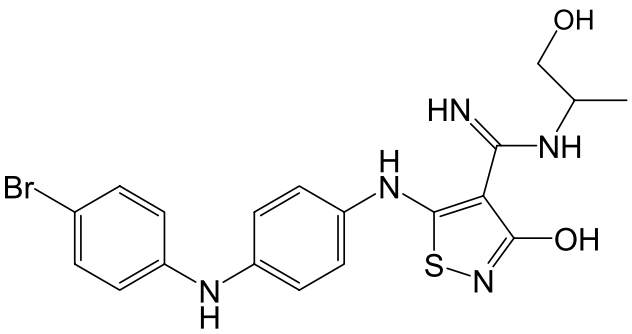

VRX 0466617
IC_{50} for CHK1 > 10 μM
IC_{50} for CHK2 = 120 nM
K_i for CHK2 = 11 nM

Figure 1. The chemical structure of VRX0466617. VRX0466617 is a novel and selective Chk2 inhibitor with an IC_{50} of 120 nmol/L. It does not inhibit Chk1 with IC_{50} > 10 μmol/L. It is ATP competitive with an inhibition constant K_i of 11 nmol/L.

inhibited both the autophosphorylation of Chk2 and the phosphorylation of Cdc25C substrate (Fig. 2A).

To evaluate the efficacy of VRX0466617 *in vivo*, kinase assays were done on Chk2 immunoprecipitated from LCL-N cells preincubated with 10 μmol/L of the compound, with and without irradiation (0 or 4 Gy). Under these conditions, VRX0466617 inhibited to some degree both the *trans* and *cis* phosphorylation activity of Chk2 (Fig. 2B). This inhibition was not complete possibly because of the dissociation of the inhibitor from Chk2 during the immunoprecipitation/kinase assay.

To further assess this inhibitory activity, we analyzed the IR-induced Ser^{387} autophosphorylation of Chk2 immunoprecipitated from LCL-N cells exposed to increasing amounts (50 nmol/L–10 μmol/L) of VRX0466617 for 2.5 h and irradiated with 4 Gy 90 min before harvesting. The results (Fig. 2C) revealed a marked suppression of the IR-induced Thr^{387} phosphorylation signal with VRX0466617 concentration ranging from 0.5 to 10 μmol/L, but not with lower doses. It should be noticed that VRX0466617 also suppressed the IR-induced mobility shift of Chk2 (Fig. 2C), an event related to its hyperphosphorylation.

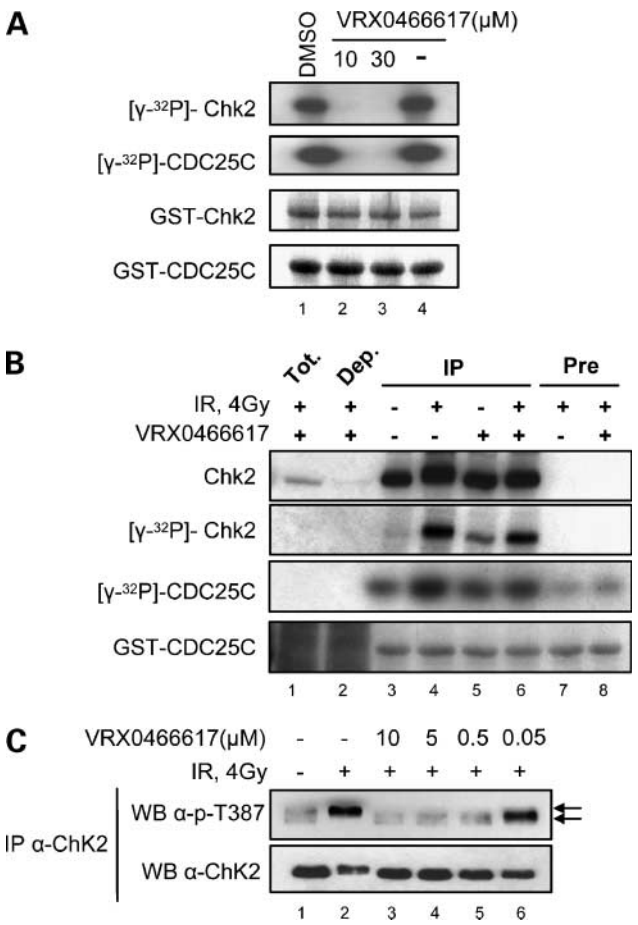

Figure 2. Inhibition of Chk2 catalytic activity *in vitro* and *in vivo* by VRX0466617. **A,** kinase-active GST-Chk2 fusion protein was tested in the presence of the indicated doses of VRX0466617 or DMSO (vehicle control) in *in vitro* kinase reaction using GST-Cdc25C as a substrate. **B,** LCL-N cells were preincubated with 10 μmol/L VRX0466617 and collected 90 min after treatment with 0 or 4 Gy IR. The endogenous Chk2 was immunoprecipitated and kinase assayed *in vitro* for *trans* and *cis* phosphorylation activity. *Tot,* total cell extract; *Dep,* Chk2-depleted extract; *IP,* Chk2 immunoprecipitate; *Pre,* precleared extract. **C,** Chk2 immunoprecipitates obtained as in (**B**) were analyzed on Western blots to evaluate the autophosphorylation of Chk2 on Ser^{387} using a phosphospecific antibody. Note that IR-induced, hyperphosphorylation-related band shift was evident only with lower doses of VRX0466617.

VRX0466617 Impairs the Phosphorylation of Chk2 Residues within the S/TQ Region

As the full activation of Chk2 in response to DNA damage involves its phosphorylation at multiple sites within the NH_2-terminal S/TQ region (21, 26), we analyzed the intracellular effect of VRX0466617 on Chk2 Ser^{19}, Ser^{33-35}, and Thr^{68}. The phosphorylation of these residues, although dependent on ATM, is differentially regulated by the yield of DNA damage, with Thr^{68} being phosphorylated by far lower radiation doses (<0.25 Gy) than those required for the phosphorylation of Ser^{19} and Ser^{33-35} (>0.5 Gy; ref. 26). The analysis at 30 min post-IR showed that 5 to 10 μmol/L VRX0466617, but not lower concentrations, markedly inhibited the phosphorylation of Ser^{33-35} and, to a less extent, of Ser^{19}, but not of Thr^{68} (Fig. 3). It is interesting that at 180 min post-IR, the presence of VRX0466617 sustained Thr^{68} phosphorylation (Fig. 3, *lanes 8* and *9*), whereas Ser^{19} and Ser^{33-35} remained unphosphorylated. Unexpectedly, VRX0466617 elevated the Thr^{68} phosphorylation of unirradiated cells (Fig. 3, *lane 3*), raising the possibility that this compound might either increase the affinity of the phosphoresidue for or facilitate the interaction with ATM; induce DNA damage, therefore activating ATM; or interfere with molecules that regulate the phosphorylation of Chk2 Thr^{68}.

The IR-Induced Responses Upstream of Chk2 Are Not Affected by VRX0466617

Besides Chk2, ATM phosphorylates several other substrates in response to DNA damage (27). To exclude any off-target effects of VRX0466617 that might affect ATM activity and thereby affect its downstream targets, we analyzed the phosphorylation of p53 Ser^{15} and Smc1 Ser^{966}, two specific substrates of ATM (2). In addition, we assessed the phosphorylation of Chk1 on Ser^{317} and Ser^{345}, which, in response to IR, is carried out by ATR in an ATM-dependent manner (28, 29). After irradiation, the phosphorylation of these residues markedly increased but was not significantly affected by treatment with up to 10 μmol/L VRX0466617 (Fig. 4A–C), thus ruling out a nonspecific effect of the compound toward ATM and ATR kinases.

It should be noticed that because Smc1, p53, or Chk1 remained unphosphorylated after treatment with VRX0466617 alone (Fig. 4A–C, *lane 3*), it is unlikely that the phosphorylation of Chk2 Thr^{68} induced by this compound could be ascribed to the activity of ATM. To exclude this, we compared the effects of VRX0466617 with those of KU-55933, a selective inhibitor of ATM kinase (12), and their combination. Whereas IR induced a marked autophosphorylation of ATM Ser^{1981} and phosphorylation of its downstream Smc1 Ser^{966}, p53 Ser^{15}, and Chk2 Thr^{68},

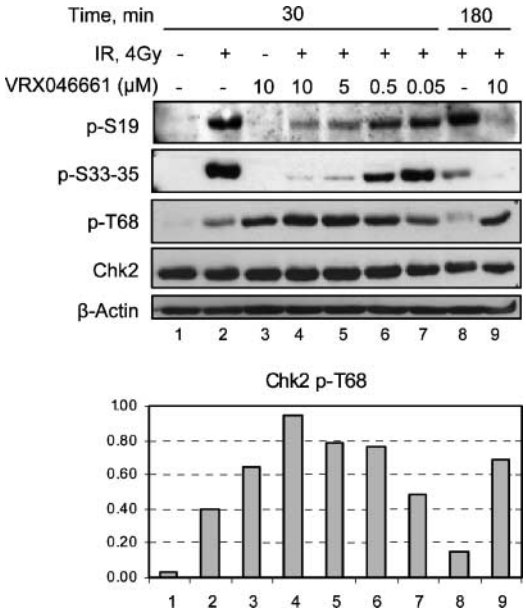

Figure 3. VRX0466617 effects on the phosphorylation of Chk2 residues within the S/TQ region. LCL-N cells preincubated for 2.5 h with different doses of VRX0466617, treated with 0 or 4 Gy IR, and harvested 30 or 180 min later. Extracts from these cells were analyzed on Western blots with Chk2 Ser^{19}, Ser^{33-35}, and Thr^{68} phosphospecific antibodies. For each lane, the relative levels of Chk2 p-Thr^{68}, normalized for those of total Chk2 and determined by densitometry analysis of the bands, are shown in the histogram (*right*). *Y-axis,* relative levels of p-Thr^{68}.

these events were, as expected, totally abrogated by KU-55933 (Fig. 5A, *lane 8*). Treatment with VRX0466617 alone markedly increased the basal phosphorylation of Chk2 Thr^{68} but not ATM Ser^{1981} (Fig. 5A, *lane 3*). More interestingly, the IR-induced phosphorylation of Chk2 Thr^{68} was not ablated by incubation with both VRX0466617 and KU-55933 (Fig. 5A, compare *lanes 6* and *8*). Altogether, the VRX0466617-induced phosphorylation of Chk2 Thr^{68} in undamaged cells seems to be ATM dependent (compare *lanes 3* and *5*) but ATM independent in DNA-damaged cells (compare *lanes 4* and *6*).

Accordingly, we found that the phosphorylations on Thr^{68} of the wild-type and kinase-dead forms of Chk2 expressed in the Chk2-deficient cell line HCT15 are markedly different (Fig. 5B). Indeed, compared with wild-type Chk2, kinase-dead Chk2 showed far higher levels of phospho-Thr^{68} before irradiation (Fig. 5B, compare *lanes 1* and *3*), consistent with the elevated Thr^{68} phosphorylation seen in cells treated with VRX0466617. This indicates that inactivation of the Chk2 enzyme, either by mutagenesis of its catalytic site or by chemical inhibition, is responsible for the induced phosphorylation of Thr^{68}. After irradiation, the Thr^{68} phosphorylation level was similar between the wild-type and kinase-dead forms of Chk2. The basal phosphorylation on Ser^{33-35} was very different between cells expressing the wild-type Chk2 and kinase-dead Chk2, but after irradiation both showed increased levels, although more markedly in the former.

Chk2 Inhibition by VRX0466617 Prevents IR-Induced Hdmx Protein Degradation

To evaluate the *in vivo* consequence of Chk2 inhibition, we analyzed Hdmx, a negative regulator of p53, which, in response to IR, is phosphorylated by Chk2 on Ser^{342} and Ser^{367}, resulting in proteolytic degradation (4, 5). IR treatment of LCL-N cells caused a marked reduction in Hdmx protein levels (Fig. 6A, compare *lanes 1* and *2*) and a concomitant increase in the phosphorylation of p53 Ser^{20}, another target of Chk2. However, the IR-induced degradation of Hdmx was, to a large extent, prevented by increasing doses of VRX0466617 (Fig. 6A, *lanes 4–7*), whereas the induction of p53 and p53 phospho-Ser^{20} was attenuated. VRX0466617 prevented the IR-induced degradation of Hdmx also in BJ-hTERT fibroblasts, although less effectively than in LCL-N cells (Fig. 6B). Experiments comparing the response of $Chk2^{+/+}$ and $Chk2^{-/-}$ HCT116 cells again showed the effectiveness of VRX0466617 in preventing IR-induced degradation of Hdmx in the former cells (Fig. 6C, compare *lanes 2* and *4*) and selectivity for Chk2, given the lack of activity in the latter cells (Fig. 6C, *lanes 6* and *8*).

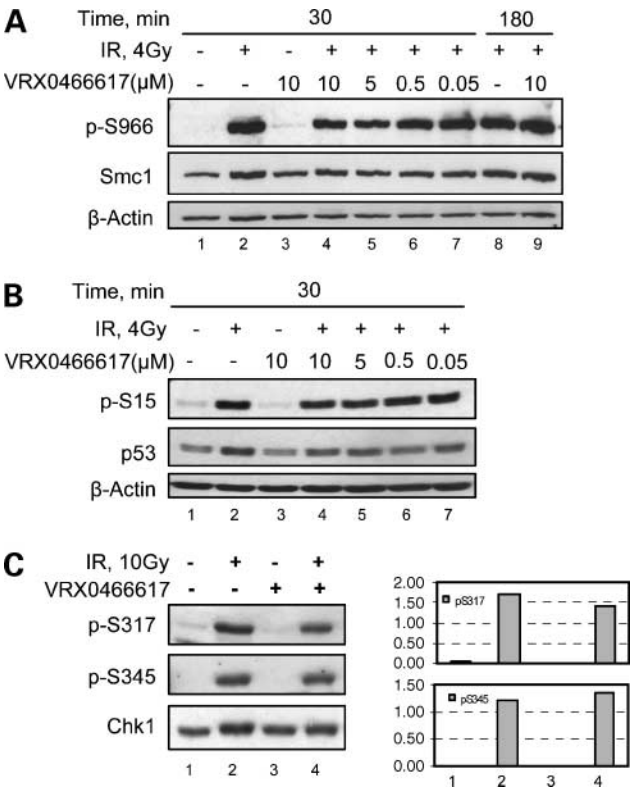

Figure 4. The phosphorylation of ATM substrates is not affected by VRX0466617. LCL-N cells were preincubated for 2.5 h with VRX0466617, treated with 0 or 4 Gy IR, and collected 30 or 180 min later. Total extracts from these cells were analyzed by Western blot with antibodies phosphospecific for Smc1 Ser^{966} (**A**), p53 Ser^{15} (**B**), and Chk1 Ser^{317} and Chk1 Ser^{345} (**C**, *left*) or recognizing the total forms of these proteins. **C,** *right,* relative levels of the phosphorylated forms of Chk1 after normalization for the total levels of Chk1, as determined by densitometry analysis of the bands of the corresponding Western blot.

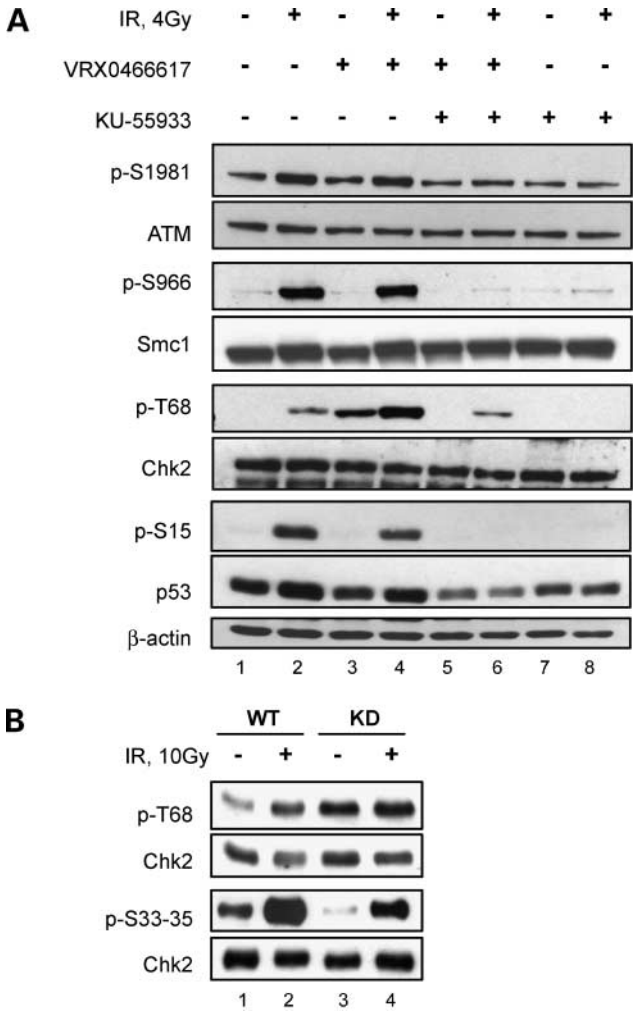

Figure 5. VRX0466617-induced Chk2 Thr^{68} phosphorylation in relation to ATM and DNA damage and enhancement by inactive Chk2. **A,** LCL-N cells were pretreated for 2.5 h with 10 μmol/L VRX0466617, for 1 h with KU-55933, or their combination. Cells were harvested 45 min after exposure to 0 or 4 Gy IR. Total lysates were Western blotted with the indicated pan-specific or phosphospecific antibodies. **B,** the Chk2-defective HCT15 cell line was transiently transfected with the hemagglutinin-tagged wild-type Chk2 (*WT*) and kinase-dead Chk2 (*KD*) forms and collected 45 min after treatment with 0 or 4 Gy IR. Total cell extracts were analyzed on Western blot with Chk2 phosphospecific antibodies or with an antihemagglutinin antibody to verify Chk2 protein loading per lane.

VRX0466617 Effects on Cell Cycle Phases, Growth, and Apoptosis

The role of Chk2 in cell cycle checkpoints prompted us to determine the effects of VRX0466617 on the cell cycle of untreated and IR-treated BJ-hTERT and LCL-N. As illustrated in Fig. 7A and summarized in Fig. 7B, the DNA flow cytometry analysis showed no significant differences in cell cycle phase distribution in the presence or absence of VRX0466617 when comparing either unirradiated or irradiated samples. To investigate the effect of Chk2 inhibition on G_2-M checkpoint, the mitotic index was measured in SAOS cells at 4 h post-IR. Compared with samples treated with DMSO (vehicle), those treated with IR alone showed a consistent reduction of the mitotic index, and similar findings were seen in samples irradiated in the presence of VRX0466617 (Fig. 7C). These findings would thus indicate that these cells possess a normal G_2-M checkpoint arrest in response to IR, not inhibited by VRX0466617.

The effects of VRX0466617 on growth were evaluated in BJ-hTERT at days 2 and 6 by microscopy enumeration of viable cells. At day 2, neither the basal nor the IR-suppressed growth was affected by the compound (Fig. 8A). At day 6, VRX0466617 induced a 45% growth reduction, relative to untreated samples, but did not potentiate the effect of IR (Fig. 8A). To determine the reason for this antiproliferative effect of VRX0466617 at day 6, we did cell cycle analysis. As shown in Fig. 8B, samples treated with VRX0466617 alone showed, compared with controls, a marked accumulation of G_2-M phase cells (G_1/G_2-M ratio, 14.7 versus 0.7), suggesting that, in the long term, Chk2 inhibition might slow down the G_2-M progression rate. However, it cannot be excluded that this G_2-M accumulation arises from an off-target effect, for instance for the mitotic kinase Aurora A toward which VRX0466617 exhibits a minor activity (see Discussion).

The possible antiapoptotic effect of 10 μmol/L VRX0466617 was determined by flow cytofluorimetry analysis of the subdiploid peak in BJ-hTERT cells treated for 2 or 6 days. The apoptotic cells, accounting in untreated controls for ~3%, increased to ~7.8% at day 2 and to 11% at day 6 in samples treated with VRX0466617 alone (Fig. 8C). However, the percentage of apoptosis at day 6 did not change in samples treated with IR plus VRX0466617, suggesting a radioprotecting effect by this compound. Because mouse thymocytes are sensitive to IR-induced apoptosis and acquire radioresistance on Chk2 deficiency (30), we studied the effects of VRX0466617 in these cells. At 24 h posttreatment with DMSO (vehicle) or 10 μmol/L VRX0466617, ~7% of apoptotic events were seen (Fig. 8D). Following treatment with 5 Gy IR, thymocytes underwent a massive apoptosis (~63%), which was attenuated (~36%) by pretreatment with VRX0466617, hence indicating that this compound affords radioprotection.

Because earlier DNA flow cytometry analysis suggested that VRX0466617 might induce hyperdiploidy, we investigated this occurrence in BJ-hTERT cultured for up to 10 days. Compared with untreated controls, VRX0466617-treated samples showed a time-dependent increase in cells with hyperdiploid (>2N) DNA content (Fig. 8E, *top*). To exclude the possibility of an artifact such as cell clumping, this population was sorted by fluorescence-activated cell sorting and analyzed by fluorescence microscopy. As shown in Fig. 8E (*bottom*), the sorted fraction only contained single multinucleated cells. Thus, VRX0466617 can, in long term, give increase to cell polyploidy.

VRX0466617 Does Not Potentiate the Cytotoxicity of Anticancer Drugs

Whether VRX0466617 potentiates the cytotoxic activity of anticancer drugs was investigated in MCF7 cells that were pretreated with or without 10 μmol/L VRX0466617 and

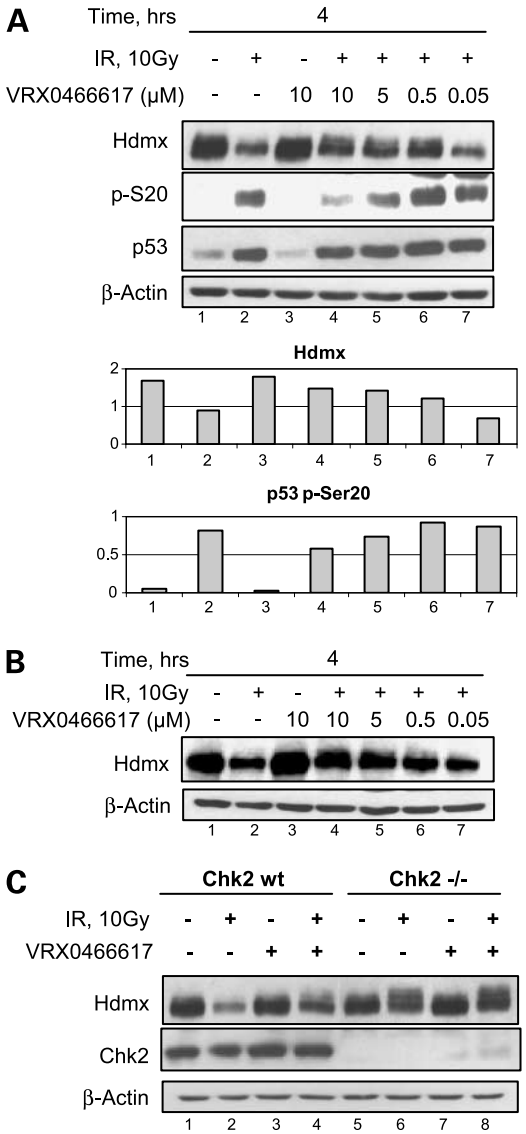

Figure 6. Effect of VRX0466617 on *in vivo* Chk2-mediated stability of Hdmx. LCL-N cells were preincubated with escalating doses of VRX0466617, harvested 4 h after irradiation with 0 or 10 Gy, and analyzed on Western blots for Hdmx, p53, and p53 phospho-Ser^{20} (**A**). For each lane, the relative levels of Hdmx and p53-pSer^{20} after normalization for β-actin, as obtained by densitometry analysis of the bands, are shown in histograms (*right*). The effect of VRX0466617 on Hdmx was examined in BJ-hTERT cells (**B**) and in wild-type and Chk2$^{-/-}$ HCT116 cells (**C**).

incubated with escalating doses of the DNA-damaging drugs doxorubicin and cisplatin. The results of the 3-(4,5-dimethylthiazol-2-yl)-2,5-diphenyltetrazolium bromide assays (Fig. 9) revealed that VRX0466617 had no effect on the cytotoxic activity of these compounds. Likewise, the cytotoxicity of doxorubicin, cisplatin, and the microtubule-binding agent Taxol in BJ-hTERT was unaffected by the presence of VRX0466617 (data not shown). Hence, VRX0466617 does not seem to modulate the killing potential of anticancer drugs.

Discussion

Inactivation of genes of the ATM/ATR–dependent DNA damage response can profoundly affect the sensitivity of normal cells and cancer cells to DNA-damaging agents and

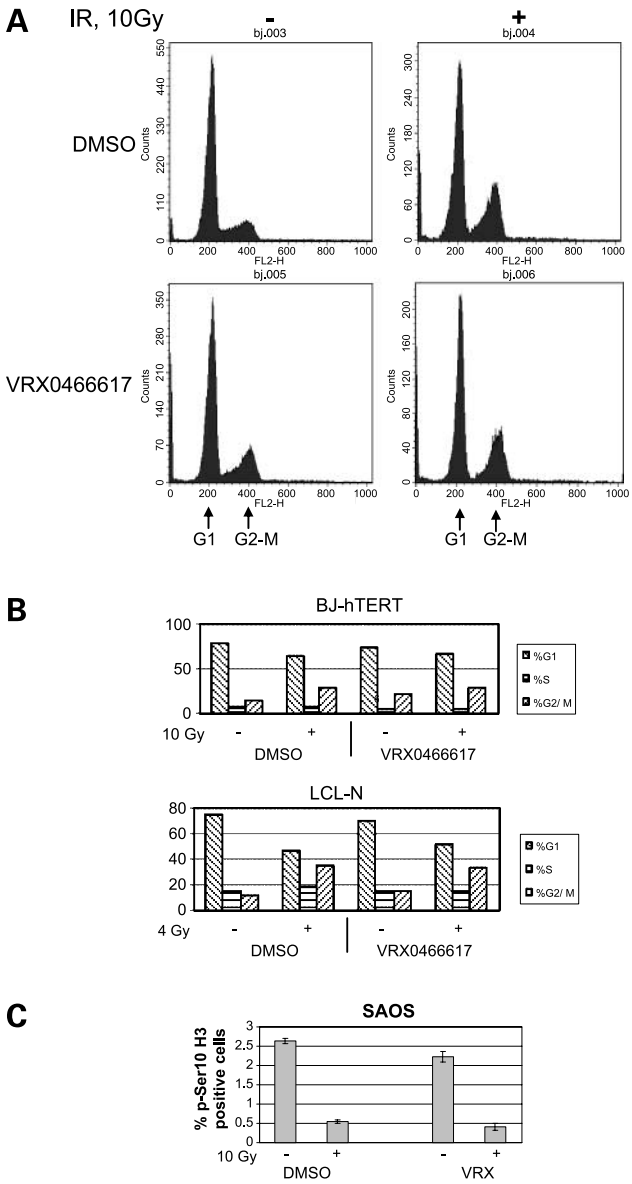

Figure 7. Cell cycle phase distribution after VRX0466617 treatment. BJ-hTERT and LCL-N cells were pretreated for 2.5 h with 10 μmol/L VRX0466617 or DMSO (vehicle), irradiated with 10 and 4 Gy, respectively, and collected after 48 h for the former and after 24 h for the latter. After fixation and staining with propidium iodide, cells were analyzed for DNA content by flow cytofluorimetry. **A,** a typical DNA profile of untreated and treated BJ-hTERT. **B,** percentage of G_1, S, and G_2-M cells per each experimental point (results from three independent experiments). **C,** SAOS cells were treated with DMSO and VRX0466617 with or without IR. Samples were preincubated with VRX0466617 for 2.5 h before treatment with 10 Gy and harvested 4 h after irradiation. Mitotic cells were detected after immunofluorescent staining of samples with an anti–phospho-histone H3 (Ser^{10}) antibody. *Columns,* mean of three independent experiments; *bars,* SD.

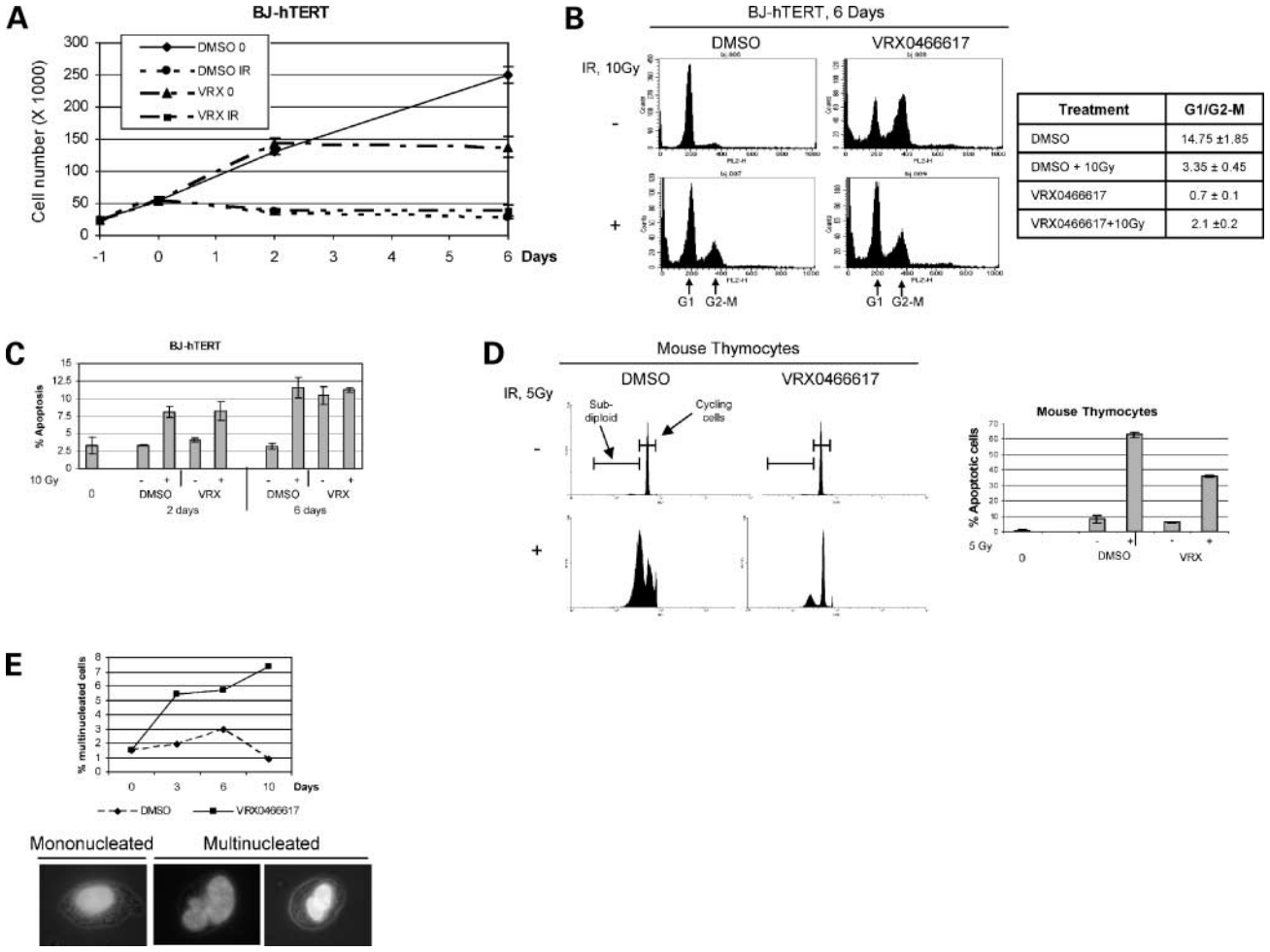

Figure 8. VRX0466617 effects on cell growth, apoptosis, and ploidy. **A,** BJ-hTERT cells were preincubated at day 0 for 2.5 h with 10 μmol/L VRX0466617 or vehicle (DMSO) and exposed to 0 or 10 Gy IR. After 2 or 6 d, cells were stained with trypan blue and viable cells scored by optical microscopy. *Points,* mean of three independent experiments; *bars,* SD. **B,** *left,* flow cytometric DNA histogram depicting the effect of VRX0466617 on BJ-hTERT cell cycle phases at day 6. The G_1/G_2-M values are also reported (*right*). **C,** amount of subdiploid apoptotic events in BJ-hTERT samples after treatment with the indicated agents. **D,** thymocytes were preincubated with VRX0466617 or DMSO (vehicle) before IR exposure and subdiploid events scored 24 h later by flow cytometry. *Left,* representative DNA histogram. *Right, columns,* mean of three independent experiments; *bars,* SD. **E,** *top,* number of multinucleated cells in BJ-hTERT at various time points after exposure to a single dose of VRX0466617. Multinucleated cells were isolated from propidium iodide–stained samples with a fluorescence-activated cell sorter equipped with an electronic doublet discrimination module (which differentiates between single cells and aggregates) and setting a fluorescence window above the 4N DNA content. *Bottom,* fluorescence microscopy analysis of fluorescence-activated cell sorted events with a DNA content >4N verified their multinucleated nature.

ionization radiation, making this checkpoint pathway an attractive pharmacologic target to intervene to enhance the efficacy of conventional antitumor chemotherapy and radiotherapy (10). This therapeutic interest has led in recent years to the development of small molecules that selectively inhibit a particular component of the DNA damage response pathway, such as ATM, ATR, or the downstream cell cycle checkpoint kinases Chk1 and Chk2 (31). Chk1 has been of particular interest as a therapeutic target because its loss of function abrogates the G_2 cell cycle arrest and sensitizes even p53-deficient cancer cells to genotoxic agents, as best attested by studies with UCN-01, a known inhibitor that is currently in phase II clinical trials for patients with advanced cancers (14).

In this study, we characterized the *in vitro* activity and cellular effects of a novel Chk2-specific inhibitor VRX0466617. Chk2 is an effector serine/threonine kinase that, in response to DNA damage, is phosphorylated by ATM on Thr^{68}. This event triggers a cascade of additional phosphorylations leading to the full activation of its enzymatic activity (21, 32). Once activated, Chk2 phosphorylates at least 10 different molecules involved in cell cycle checkpoint arrest (e.g., Cdc25C), DNA repair (e.g., BRCA1), apoptosis (e.g., E2F-1 and p53), and circadian clock signaling (e.g., Per1; refs. 33, 34).

We have shown that VRX0466617 inhibits both the *trans* and *cis* phosphorylation of recombinant Chk2. Moreover, it significantly suppresses the *in vivo* DNA damage–induced

intracellular activation of Chk2. We have shown that when cells are pretreated with 10 μmol/L VRX0466617, the radiation-induced autophosphorylation of Chk2 and the phosphorylation of the Cdc25C substrate are both suppressed, as evident from *in vitro* kinase assay with Chk2 immunoprecipitates. Moreover, dose-dependent experiments have shown that 5 to 10 μmol/L of VRX0466617 markedly inhibit the intracellular autophosphorylation of Chk2 on Thr^{387}.

Although the phosphorylation of Thr^{68} by ATM is essential for Chk2 activation, two other recently identified phosphoresidues, Ser^{19} and Ser^{33-35}, participate in this process (26). We have therefore examined the *in vivo* effect of VRX0466617 on these phosphoryl residues and showed that it inhibits, in a dose-dependence manner, the induced phosphorylation of Ser^{19} and Ser^{33-35}, but not of Thr^{68}. Surprisingly, even in undamaged cells, VRX0466617 enhanced the phosphorylation of Chk2 Thr^{68}, suggesting a few possibilities that could underlie this phenomenon. There are several lines of evidence for the activation of ATM by drugs that cause chromatin conformation changes without inducing physical damage to DNA (35). We excluded an activation of ATM by VRX0466617 because in cells treated with this compound, neither the ATM targets Smc1 Ser^{966} and p53 Ser^{15} nor the ATM/ATR targets Chk1 Ser^{317} and Chk1 Ser^{345} seemed to be phosphorylated. In light of the fact that even a kinase-dead form of Chk2 shows constitutive phosphorylation on Thr^{68} in unstressed cells, it might be hypothesized the existence of an activation mechanism that negatively regulates the phosphorylation of Thr^{68} possibly through a phosphatase itself dependent on the basal activity of Chk2. In accordance with this, it has been recently shown that the protein phosphatase 2A interacts with and regulates Chk2 activation by dephosphorylation (36). Obviously, more work is needed to elucidate this drug-activated Thr^{68} phosphorylation mechanism.

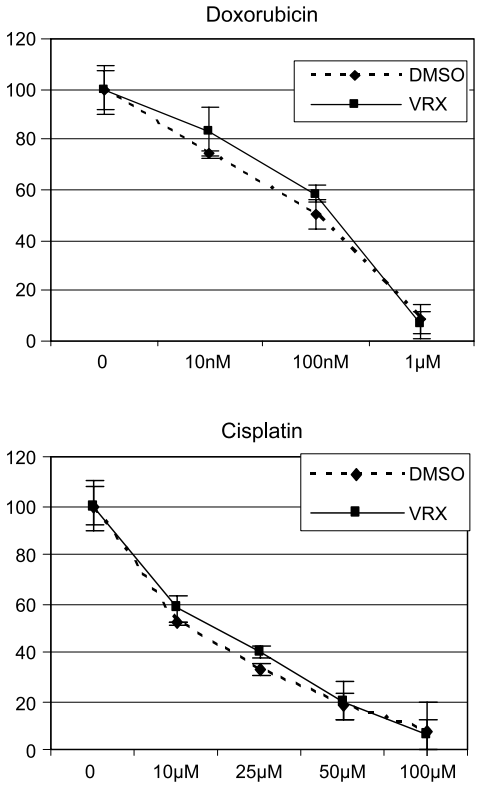

Figure 9. Combined effects of VRX0466617 with anticancer drugs. MCF7 cells were seeded in 96-well plates; pretreated for 2.5 h with 10 μmol/L VRX0466617 before addition of the indicated doses of doxorubicin, Taxol, and cisplatin; and incubated for 72 h. Cell proliferation was determined by the 3-(4,5-dimethylthiazol-2-yl)-2,5-diphenyltetrazolium bromide assay. For a given dose of treatment, growth values (*Y axis*) were normalized to those of untreated cells. *Points,* mean of three independent experiments; *bars,* SD.

In response to DNA damage, both ATM and Chk2 phosphorylate the negative regulator of p53 Hdmx at multiple residues, leading to Hdmx-mediated ubiquitination and degradation (4, 5). We therefore analyzed the functional effect *in vivo* of Chk2 inhibition in three different cell lines and showed that VRX0466617 prevents, in a dose-dependent manner, the degradation of Hdmx. Together with the fact that this effect is not seen in Chk2-null cells, these findings further highlight the specificity and functional activity of VRX0466617 *in vivo*.

VRX0466617 did not significantly perturb in short-term culture the cell cycle distribution and G_2-M arrest of unirradiated and irradiated cells, a somewhat unexpected finding given the ascribed role for Chk2 in cell cycle checkpoints (3). This observation, however, is in accordance with studies of embryonic fibroblasts from Chk2-null mice showing a slightly impaired G_1 checkpoint but neither S nor G_2-M checkpoint defects in response to IR (30, 37). These findings are in contrast to the effects of the ATM inhibitor KU-55933 and Chk1 inhibitor UCN-01, which cause marked cell cycle phase changes following IR treatment (data not shown). In long-term (>6 days) but not short-term (<2 days) culture, VRX0466617 exhibited an antiproliferative effect, which was paralleled by an accumulation of G_2-M phase cells, implying that the chemical inhibition of Chk2 slows down the rate of G_2-M progression of cells that have undergone at least one division cycle. However, given the off-target, albeit modest, effect of VRX0466617 against the mitotic kinase Aurora A whose chemical inhibition causes accumulation of cells with >4N DNA content (38), it cannot be excluded that the G_2-M accumulation, as well as aneuploidy, might arise from this nonspecific activity of VRX0466617. This off-target effect of VRX0466617 for Aurora A could also explain the increased apoptosis of BJ-hTERT at day 6 of treatment (Fig. 8C), given that one of the cellular consequences of Aurora inhibition is indeed apoptosis (38).

A major feature of Chk2-null mice and cells derived from these animals is their increased resistance to genotoxic agents, associated with reduced transcriptional induction of p53-dependent genes, such as *p21* and *Noxa*. In support of this, an ATP-competitive Chk2 inhibitor, compound 19 (17), was recently shown to provide a dose-dependent protection of T lymphocytes against apoptosis, suggesting a

radioprotective role by this compound. Interestingly, we also showed that VRX0466617 exhibits some level of radioprotection, as evidenced in BJ-hTERT cells at 6 days and more significantly in mouse thymocytes at 24 h post-IR. The modest differences in apoptotic events seen in BJ-hTERT cells 2 or 6 days after treatment might be explained by the redundancy of checkpoint pathways present in normal cells that could mask any checkpoint defect introduced by VRX0466617. Because VRX0466617 did not modify the cytotoxicity of anticancer drug doxorubicin, cisplatin, and Taxol, it seems that the catalytic activity of Chk2 may not be a crucial determinant for killing of cancer cells.

In conclusion, we have shown that VRX0466617 selectively blocks the intracellular catalytic activity of Chk2 without interfering with the upstream ATM/ATR pathway. This pharmacological inhibition prevents the degradation of Hdmx and attenuates the genotoxic response. These results underscore the specificity of VRX0466617 for Chk2 *in vivo* and support the use of this compound as a biological probe to study and dissect the Chk2-dependent pathways.

References

1. Kastan MB, Bartek J. Cell-cycle checkpoints and cancer [review]. Nature 2004;432:316 – 23.

2. Shiloh Y. The ATM-mediated DNA-damage response: taking shape. Trends Biochem Sci 2006;31:402 – 10.

3. Bartek J, Lukas J. Chk1 and Chk2 kinases in checkpoint control and cancer [review]. Cancer Cell 2003;3:421 – 9.

4. Chen L, Gilkes DM, Pan Y, Lane WS, Chen J. ATM and Chk2-dependent phosphorylation of MDMX contribute to p53 activation after DNA damage. EMBO J 2005;24:3411 – 22.

5. Okamoto K, Kashima K, Pereg Y, et al. DNA damage-induced phosphorylation of MdmX at serine 367 activates p53 by targeting MdmX for Mdm2-dependent degradation. Mol Cell Biol 2005;25:9608 – 20.

6. Stevens C, Smith L, La Thangue NB. Chk2 activates E2F-1 in response to DNA damage. Nat Cell Biol 2003;5:401 – 9.

7. Rogoff HA, Pickering MT, Frame FM, et al. Apoptosis associated with deregulated E2F activity is dependent on E2F1 and Atm/Nbs1/Chk2. Mol Cell Biol 2004;24:2968 – 77.

8. Zhang J, Willers H, Feng Z, et al. Chk2 phosphorylation of BRCA1 regulates DNA double-strand break repair. Mol Cell Biol 2004;24:708 – 18.

9. Yang S, Kuo C, Bisi JE, Kim MK. PML-dependent apoptosis after DNA damage is regulated by the checkpoint kinase hCds1/Chk2. Nat Cell Biol 2002;4:865 – 70.

10. Zhou BB, Bartek J. Targeting the checkpoint kinases: chemosensitization versus chemoprotection. Nat Rev Cancer 2004;4:216 – 25.

11. Cowell IG, Durkacz BW, Tilby MJ. Sensitization of breast carcinoma cells to ionizing radiation by small molecule inhibitors of DNA-dependent protein kinase and ataxia telangiectsia mutated. Biochem Pharmacol 2005; 71:13 – 20.

12. Hickson I, Zhao Y, Richardson CJ, et al. Identification and characterization of a novel and specific inhibitor of the ataxia-telangiectasia mutated kinase ATM. Cancer Res 2004;64:9152 – 9.

13. Busby EC, Leistritz DF, Abraham RT, Karnitz LM, Sarkaria JN. The radiosensitizing agent 7-hydroxystaurosporine (UCN-01) inhibits the DNA damage checkpoint kinase hChk1. Cancer Res 2000;60:2108 – 12.

14. Hotte SJ, Oza A, Winquist EW, et al. Phase I trial of UCN-01 in combination with topotecan in patients with advanced solid cancers: a Princess Margaret Hospital Phase II Consortium study. Ann Oncol 2006; 17:334 – 40.

15. Kohn EA, Yoo CJ, Eastman A. The protein kinase C inhibitor Go6976 is a potent inhibitor of DNA damage-induced S and G_2 cell cycle checkpoints. Cancer Res 2003;63:31 – 5.

16. Syljuasen RG, Sorensen CS, Nylandsted J, Lukas C, Lukas J, Bartek J. Inhibition of Chk1 by CEP-3891 accelerates mitotic nuclear fragmentation in response to ionizing radiation. Cancer Res 2004;64:9035 – 40.

17. Arienti KL, Brunmark A, Axe FU, et al. Checkpoint kinase inhibitors: SAR and radioprotective properties of a series of 2-arylbenzimidazoles. J Med Chem 2005;48:1873 – 85.

18. Buscemi G, Perego P, Carenini N, et al. Activation of ATM and Chk2 kinases in relation to the amount of DNA strand breaks. Oncogene 2004; 23:7691 – 700.

19. Jallepalli PV, Lengauer C, Vogelstein B, Bunz F. The Chk2 tumor suppressor is not required for p53 responses in human cancer cells. J Biol Chem 2003;278:20475 – 9.

20. Zannini L, Lecis D, Lisanti S, et al. Karyopherin-α2 protein interacts with Chk2 and contributes to its nuclear import. J Biol Chem 2003;278: 42346 – 51.

21. Buscemi G, Savio C, Zannini L, et al. Chk2 activation dependence on Nbs1 after DNA damage. Mol Cell Biol 2001;21:5214 – 22.

22. Delia D, Mizutani S, Tagliabue E, et al. ATM protein and p53 serine 15 phosphorylation in Ataxia Telangiectasia (AT) patients and AT heterozygotes. Br J Cancer 2000;82:1938 – 45.

23. Xu B, Kim ST, Lim DS, Kastan MB. Two molecularly distinct G_2/M checkpoints are induced by ionizing irradiation. Mol Cell Biol 2002;22: 1049 – 59.

24. Varaprasad C, Barawkar D, Abdellaoui H, et al. Discovery of 3-hydroxy-4-carboxyalkylamidino-5-arylamino-isothiazoles as potent MEK1 inhibitors. Bioorg Med Chem Lett 2006;16:3975 – 80.

25. Larson G, Yan S, Chen H, et al. Identification of novel, selective and potent Chk2 inhibitors. Bioorg Med Chem Lett 2007;17:172 – 5. Epub 2006 Oct 10.

26. Buscemi G, Carlessi L, Zannini L, et al. DNA damage-induced cell cycle regulation and function of novel Chk2 phosphoresidues. Mol Cell Biol 2006;26:7832 – 45.

27. Lavin MF, Delia D, Chessa L. ATM and the DNA damage response. Workshop on ataxia-telangiectasia and related syndromes. EMBO Rep 2006;7:154 – 60.

28. Jazayeri A, Falck J, Lukas C, et al. ATM- and cell cycle-dependent regulation of ATR in response to DNA double-strand breaks. Nat Cell Biol 2006;8:37 – 45.

29. Cuadrado M, Martinez-Pastor B, Murga M, et al. ATM regulates ATR chromatin loading in response to DNA double-strand breaks. J Exp Med 2006;203:297 – 303.

30. Takai H, Naka K, Okada Y, et al. Chk2-deficient mice exhibit radioresistance and defective p53-mediated transcription. EMBO J 2002; 21:5195 – 205.

31. Collins I, Garrett MD. Targeting the cell division cycle in cancer: CDK and cell cycle checkpoint kinase inhibitors [review]. Curr Opin Pharmacol 2005;5:366 – 73.

32. Matsuoka S, Huang M, Elledge SJ. Linkage of ATM to cell cycle regulation by the Chk2 protein kinase. Science 1998;282:1893 – 7.

33. Pommier Y, Sordet O, Rao VA, Zhang H, Kohn KW. Targeting chk2 kinase: molecular interaction maps and therapeutic rationale [review]. Curr Pharm Des 2005;11:2855 – 72.

34. Gery S, Komatsu N, Baldjyan L, Yu A, Koo D, Koeffler HP. The circadian gene per1 plays an important role in cell growth and DNA damage control in human cancer cells. Mol Cell 2006;22:375 – 82.

35. Bakkenist CJ, Kastan MB. DNA damage activates ATM through intermolecular autophosphorylation and dimmer dissociation. Nature 2003;421:499 – 506.

36. Liang X, Reed E, Yu JJ. Protein phosphatase 2A interacts with Chk2 and regulates phosphorylation at Thr-68 after cisplatin treatment of human ovarian cancer cells. Int J Mol Med 2006;17:703 – 8.

37. Jack MT, Woo RA, Hirao A, Cheung A, Mak TW, Lee PW. Chk2 is dispensable for p53-mediated G_1 arrest but is required for a latent p53-mediated apoptotic response. Proc Natl Acad Sci U S A 2002;99:9825 – 9.

38. Harrington EA, Bebbington D, Moore J, et al. VX-680, a potent and selective small-molecule inhibitor of the Aurora kinases, suppresses tumor growth *in vivo*. Nat Med 2004;10:262 – 7.

Molecular Cancer Therapeutics

Biochemical and cellular characterization of VRX0466617, a novel and selective inhibitor for the checkpoint kinase Chk2

Luigi Carlessi, Giacomo Buscemi, Gary Larson, et al.

Mol Cancer Ther 2007;6:935-944.